NIH Public Access
Author Manuscript
Neuron. Author manuscript; available in PMC 2015 March 05.

Published in final edited form as:
Neuron. 2014 March 5; 81(5): 1111–1125. doi:10.1016/j.neuron.2014.01.012.

Multiple Mechanistically Distinct Modes of Endocannabinoid Mobilization at Central Amygdala Glutamatergic Synapses

Teniel S. Ramikie[1,3], **Rita Nyilas**[4], **Rebecca J. Bluett**[1,3], **Joyonna C. Gamble-George**[1,3], **Nolan D. Hartley**[1], **Ken Mackie**[5], **Masahiko Watanabe**[6], **István Katona**[4], and **Sachin Patel**[1,2,3,*]

[1]Department of Psychiatry Vanderbilt University School of Medicine, Nashville, TN 37212, USA

[2]Department of Molecular Physiology & Biophysics Vanderbilt University School of Medicine, Nashville, TN 37212, USA

[3]Vanderbilt Brain Institute Vanderbilt University School of Medicine, Nashville, TN 37212, USA

[4]Momentum Laboratory of Molecular Neurobiology, Institute of Experimental Medicine, Hungarian Academy of Sciences, Budapest, Hungary

[5]Gill Institute and Department of Psychological and Brain Sciences, Indiana University, Bloomington, IN 47405, USA

[6]Department of Anatomy, Hokkaido University Graduate School of Medicine, Sapporo, Japan

SUMMARY

The central amygdala (CeA) is a key structure at the limbic-motor interface regulating stress-responses and emotional learning. Endocannabinoid (eCB) signaling is heavily implicated in the regulation of stress-response physiology and emotional learning processes; however, the role of eCBs in the modulation of synaptic efficacy in the CeA is not well understood. Here we describe the subcellular localization of CB_1 cannabinoid receptors and eCB synthetic machinery at glutamatergic synapses in the CeA and find that CeA neurons exhibit multiple mechanistically and temporally distinct modes of postsynaptic eCB mobilization. These data identify a prominent role for eCBs in the modulation of excitatory drive to CeA neurons and provide insight into the mechanisms by which eCB signaling and exogenous cannabinoids could regulate stress-responses and emotional learning.

INTRODUCTION

The central amygdala (CeA) plays a key role in emotional learning processes (Ehrlich et al., 2009; Pape and Pare, 2010). Perhaps most well-studied is the role the CeA plays in unconditioned and conditioned fear generation (Ciocchi et al., 2010; Li et al., 2013; Tye et al., 2011), fear extinction and conditioned inhibition (Amano et al., 2010), as well as conditioned orienting responses to emotionally salient stimuli (El-Amamy and Holland, 2007; Groshek et al., 2005). The CeA is a subcortical structure composed of GABAergic

© 2014 Elsevier Inc. All rights reserved

*Correspondence: Sachin Patel, MD, PhD Assistant Professor Departments of Psychiatry and Molecular Physiology & Biophysics Robinson Research Building, Rm 724B Vanderbilt University Medical Center Nashville, TN 37232, USA sachin.patel@vanderbilt.edu p: (615) 936-7768 f: (615) 322-1462.

Publisher's Disclaimer: This is a PDF file of an unedited manuscript that has been accepted for publication. As a service to our customers we are providing this early version of the manuscript. The manuscript will undergo copyediting, typesetting, and review of the resulting proof before it is published in its final citable form. Please note that during the production process errors may be discovered which could affect the content, and all legal disclaimers that apply to the journal pertain.

NIH-PA Author Manuscript
NIH-PA Author Manuscript
NIH-PA Author Manuscript

NIH-PA Author Manuscript

NIH-PA Author Manuscript

NIH-PA Author Manuscript

neurons and divided into lateral (CeAL) and medial (CeAM) subdivisions (Cassell et al., 1999). The CeAL acts as the primary input nucleus of the CeA and receives strong glutamatergic drive from cortical (McDonald et al., 1999), thalamic (Li and Kirouac, 2008), as well as intra-amygdala and brainstem sources (Dong et al., 2010), and projects GABAergic axon terminals to the CeAM (Sun et al., 1994). The CeAM, in turn, projects to downstream regions involved in the expression of fear and arousal responses to salient stimuli (Davis, 1997). Functional studies have recently shown that activation of CeAL projection neurons strongly inhibits CeAM output neurons and reduces behavioral fear and anxiety responses (Ciocchi et al., 2010; Li et al., 2013; Tye et al., 2011). Thus, enhanced inhibitory control of CeAM neurons by elevated activity of CeAL projection cells may serve to constrain conditioned fear and anxiety (Amano et al., 2010; Ciocchi et al., 2010). Taken together, these data suggest that understanding the synaptic mechanisms regulating excitatory drive to CeAL neurons could provide significant insight into the mechanisms regulating the expression of fear and anxiety.

Endocannabinoids are a class of bioactive lipids produced by neurons and glia (Kano et al., 2009). 2-arachidonoylglycerol (2-AG) is thought to be the primary eCB that mediates retrograde synaptic signaling at central synapses (Castillo et al., 2012). 2-AG is post-synaptically synthesized by diacylglycerol lipase α (DAGLα) via calcium- and Gq-protein-coupled receptor (GqPCR)-dependent mechanisms (Hashimotodani et al., 2007; Hashimotodani et al., 2005; Ohno-Shosaku et al., 2005; Ohno-Shosaku et al., 2012). In contrast to 2-AG, the mechanisms regulating synaptic anandamide (AEA) synthesis are not well understood, but can involve GqPCR activation (Chavez et al., 2010; Grueter et al., 2010; Huang and Woolley, 2012). Once produced, 2-AG and AEA are primarily degraded by monoacylglycerol lipase and fatty acid amide hydrolase, respectively (Cravatt et al., 2001; Dinh et al., 2002; Long et al., 2009).

Despite the prominent role of eCB signaling in the regulation of fear, anxiety, and stress responses (Hill et al., 2010; Lutz, 2007; Ramikie and Patel, 2011; Riebe et al., 2012), the role of eCB signaling in the modulation of CeA circuitry has been relatively under-investigated due to anatomical studies that demonstrated very weak CB_1 receptor immunoreactivity within the CeA (Kamprath et al., 2011; Katona et al., 2001). Here we utilized new reagents to reveal abundant expression of eCB signaling elements at CeAL glutamatergic synapses and elucidate several mechanistically and temporally dissociated distinct modes of postsynaptic eCB mobilization in CeAL neurons subserving eCB-mediated synaptic depression of CeAL glutamatergic neurotransmission.

RESULTS

Localization of Endocannabinoid Signaling Machinery in the CeAL

Although prior studies suggested a negligible role for eCBs in the modulation of CeA synaptic signaling (Katona et al., 2001), our *in situ* hybridization studies revealed a detectable CB_1 *in situ* signal within the CeA, and strong expression in the basolateral amygdala (BLA) of wild-type, but not CB_1 knockout (KO; $CB_1^{-/-}$), mice (Figure 1A–C). The presence of CB_1 mRNA in the majority of BLA neurons, which project glutamatergic afferents to the CeAL, suggested that BLA-CeA glutamatergic terminals might express CB_1 receptor protein (Figure 1C). Therefore, we employed a new high affinity anti-CB_1 antibody to probe the localization of CB_1 receptors in the CeA (Yoshida et al., 2011). Using this antibody, CB_1 receptors were clearly detected at high levels in both the CeAL and CeAM of wild type, but not $CB_1^{-/-}$ mice (Figure 1D–F). Additionally, electron microscopic (EM) examination revealed CB_1 receptor expression in presynaptic boutons forming asymmetric synapses onto dendritic shafts and spines within the CeAL (Figure $1G_{1-2}$ and I).

NIH-PA Author Manuscript

NIH-PA Author Manuscript

NIH-PA Author Manuscript

Considering that 2-AG is the primary ligand mediating eCB retrograde signaling at central synapses, we next examined the expression of the 2-AG synthesizing enzyme, DAGLα, in the CeA. *In situ* hybridization confirmed the expression of DAGLα in both the BLA and CeA (Figure 2A–C). Immunohistochemistry, using an anti-DAGLα antibody whose specificity in the forebrain has been confirmed in DAGLα$^{-/-}$ mice (Ludanyi et al., 2011), uncovered a punctate staining pattern throughout the CeAL (Figure 2D–E). Double immunofluorescence labeling and confocal microscopy revealed DAGLα-positive puncta in close apposition to MAP2 labeled dendritic shafts in the CeAL (Figure 2F–H), suggestive of DAGLα localization in pre- or postsynaptic compartments. To differentiate between these two possibilities, we performed immunoperoxidase labeling and utilized EM to visualize DAGLα at the synaptic level. We found that DAGLα was indeed localized postsynaptically in dendritic shafts and spine heads forming asymmetric synapses in the CeAL (Figure 2I–L). Taken together these data demonstrate the presence of eCB signaling elements at glutamatergic synapses in the CeAL.

CB_1 Receptors Modulate Glutamate Release onto CeAL Neurons

To determine the functional significance of CB_1 receptor expression in the CeAL, we conducted whole-cell voltage-clamp electrophysiological recordings in the presence of picrotoxin (25–50μM) to isolate glutamatergic currents. Consistent with the localization of CB_1 receptors on excitatory axon terminals in the CeAL, we found that activation of CB_1 receptors with the cannabinoid agonist CP55940 (5μM) significantly depressed eEPSC amplitude to 52±4% of baseline in CeAL neurons from wild-type (WT) mice; an effect absent in cells from $CB_1^{-/-}$ mice (WT 52.47±3.94% vs. $CB_1^{-/-}$ 114±8%; $t(8)=7.18$, $p<0.0001$; Figure 3A–B). No significant effect on PPR was observed following 5μM CP55940 application to WT or $CB_1^{-/-}$ cells (normalized PPR: WT 1.06±0.06 vs. $CB_1^{-/-}$ 0.89±0.06; $t(8)=2$, $p=0.08$; Figure 3C). However, analysis of spontaneous EPSCs (sEPSCs) revealed a selective effect of 5μM CP55940 to reduce sEPSC frequency (vehicle 4.35±0.92 Hz vs. CP55940 1.59±0.27 Hz; $U=50.00$, $p=0.008$), but not amplitude (vehicle 20.99±1.00 pA vs. CP55940 22.80±2.20 pA; $U=9$, $p=0.32$; Figure 3D–F), by Mann-Whitney U-test.

Although the selective effect of CP55940 on frequency, but not amplitude, of sEPSCs suggests a presynaptic locus of action, the lack of effect on PPR was surprising. Therefore, we evaluated the effects of 2-AG-ether, a metabolically stable analog of 2-AG to better elucidate the mechanisms by which eCB signaling (Hanus et al., 2001), rather than a synthetic agonist, modulates glutamate release. Indeed, 50 μM 2-AG-ether caused robust synaptic depression (baseline 100.3±1.2% vs. 2-AG-ether 49.1±9.5%; $t(3)=6.13$, $p<0.01$ by paired *t*-test; Figure 3G) that was associated with a significant increase in PPR ($t(3)=3.9$, $p<0.05$ by paired *t*-test; Figure 3G inset). These data indicate that CB_1 receptors function to suppress glutamate release onto CeAL neurons.

Since CB_1 receptors in other brain regions robustly modulate GABAergic transmission (Castillo et al., 2012; Kano et al., 2009), we also tested the effects of CP55940 (5μM) on GABAergic currents in the CeAL recorded in the presence of CNQX (20μM) and AP-5 (50μM). Generally consistent with our previous report (Katona et al., 2001), and our electron microscopic observation of only a few CeAL GABAergic terminals being CB_1-positive (Figure 1G_1–G_2 and H), the effects on GABAergic transmission were small and inconsistent (baseline 100.0±0.0% vs. 76.1±9.3%; $t(7)=2.6$, $p<0.05$; Figure 3H). When compared to the effects of CP55940 (5μM) on glutamatergic transmission (from CeAL cells depicted in Fig. 3B), CP55940-induced depression of GABAergic transmission showed a significantly greater variance compared to effects on glutamate release (F-test to compare variances, $p<0.05$; Figure 3I). These data suggest that the major role of CB_1 signaling in the

NIH-PA Author Manuscript

NIH-PA Author Manuscript

NIH-PA Author Manuscript

CeAL is to broadly regulate glutamatergic transmission, while synapse- or cell type-specific modulation of GABAergic transmission may also occur.

Ca^{2+}-Driven eCB Release in the CeAL

We next examined whether CeAL glutamatergic synapses express depolarization-induced suppression of excitation (DSE), a Ca^{2+}-DAGLα-dependent form of 2-AG-mediated eCB retrograde signaling (Ohno-Shosaku et al., 2012). Two-way ANOVA revealed a significant effect of DSE (depolarization) and postsynaptic depolarization duration (Figure 3J–L). Post-hoc Sidak's analysis revealed depolarization of CeAL neurons from −70 to 0 mV resulted in a transient depression of eEPSC amplitude that was significantly different from corresponding baseline values after 5 ($p<0.001$) and 10 seconds ($p<0.001$) of postsynaptic depolarization. One-way ANOVA followed by Dunnett's post hoc analysis revealed that CeAL 10 second DSE was blocked by the CB_1 receptor antagonist, SR141716 (control 77.65±2.06% vs. 5μM SR141716 95.84±4.84%, $p<0.001$; Figure 3M–O) and absent in $CB_1^{-/-}$ mice ($CB_1^{-/-}$ 102.5±3.84%, $p<0.0001$; Figure 3O). DSE was also blocked by the DAGL inhibitor THL (10μM THL 91.20±2.13%, $p<0.05$; Figure 3O) and postsynaptic calcium chelation with 40mM BAPTA (BAPTA 92.07±1.46%, $p<0.05$; Figure 3O), indicating that Ca^{2+}-driven short-term eCB mobilization at CeAL glutamatergic synapses is mediated by 2-AG activation of CB_1 receptors. Intracellular loading of BAPTA alone did not affect frequency or amplitude of eEPSCs in CeAL neurons (control frequency 4.35±0.9 Hz vs. BAPTA 4.1±1.0 Hz, $p>0.05$; control amplitude 21.0±1.0 pA vs. BAPTA 25.1±2.6, $p>0.05$; Figure S1).

Ca^{2+}-Assisted-mACh-Receptor Driven eCB Release in the CeAL

In addition to Ca^{2+}-dependent eCB release, Gq-receptor-driven eCB mobilization is a common feature of central synapses (Katona and Freund, 2012). For example, in the hippocampus, activation of Gq-coupled M_1/M_3 muscarinic acetylcholine receptors (mAChRs) has been shown to mobilize eCB signaling in a calcium-independent manner (Kim et al., 2002; Straiker and Mackie, 2007). Importantly, mAChRs are also highly expressed in the CeAL (Roozendaal et al., 1997; van der Zee et al., 1997). To determine whether activation of mAChRs drives eCB mobilization in the CeAL, we first sought to examine the functional effects of mAChR activation on CeAL glutamatergic transmission. Experimental results from CeAL field potential recordings (fEPSPs) demonstrated that bath application of the mAChR agonist, Oxo-M (1±M), reduced the amplitude of fEPSPs to 44.40±3.69% of baseline (baseline 100.90±1.18% vs. maximal Oxo-M-induced depression 44.40±3.69%, $p<0.0001$ by paired t-test; Figure 4A), an effect that reversed following drug washout (baseline 100.90±1.18% vs. post Oxo-M washout 96.14±7.13%, $p=0.79$ by paired t-test; Figure 4A). To test whether this Oxo-M induced depression was mediated by mAChR activation we bath applied 1±M atropine, a non-selective mAChR antagonist, prior to and during Oxo-M (1±M) application. Atropine application completely blocked the effect of 1±M Oxo-M on fEPSPs (baseline 100.3±0.79% vs. atropine+Oxo-M 96.47±4.38%, $p=0.87$ by paired *t*-test; Figure 4A). Using whole-cell recordings we found that Oxo-M caused robust depression of eEPSC amplitude, an effect reduced by the M_1-preferring antagonist, pirenzepine (1±M; $p<0.0001$) and eliminated by the M_3-preferring antagonist 4-DAMP (500 nM, $p<0.0001$; Figure. 4B). Oxo-M-induced synaptic depression was associated with a large increase in PPR, which was attenuated by pirenzepine ($p<0.001$) and blocked by 4-DAMP ($p<0.0001$; Figure 4C), suggesting Oxo-M induced synaptic depression is mediated by $M_{1/3}$ receptor activation and expressed presynaptically. Importantly, neither pirenzepine nor 4-DAMP exerted any effects on glutamatergic transmission when applied alone to control CeAL slices (Figure S2). Additionally, our immunofluorescence confocal microscopy data revealed a moderate expression of the M_1 receptor subtype throughout the CeAL (Figure 4E1–E2). At high magnification, M_1 staining appears as tiny puncta closely apposed to, but

NIH-PA Author Manuscript

NIH-PA Author Manuscript

NIH-PA Author Manuscript

not overlapping with, MAP2-positve dendrites and perikarya. Together, these data demonstrate the presence of functional $M_{1/3}$ mAChRs in the CeAL.

Given the functional presence of $M_{1/3}$ mAChRs at CeAL glutamatergic synapses, we next evaluated the presence of mAChR-driven eCB release at excitatory synapses within the CeAL. It has been previously reported that DSE is effectively enhanced by the coincidental activation of Gq-coupled receptors, such as M_1/M_3 receptors, via a mechanism involving Ca^{2+} enhancement of PLC β activity (Hashimotodani et al., 2005; Kim et al., 2002; Narushima et al., 2006). Consistent with the presence of Ca^{2+}-assisted-Gq-receptor driven eCB mobilization, our results revealed that Oxo-M (1±M) pre-incubation significantly enhanced 10s DSE as compared to DSE examined under control conditions (control DSE 84.82±3.0% vs. Oxo-M DSE 60.72±5.76%; t(18)=4.1, p<0.001; Figure 4F and H). DSE under control and Oxo-M conditions were both associated with increases in PPR (p<0.05 and p<0.01 respectively by paired t-test; Oxo-M DSE PPR is significantly greater than control DSE PPR p<0.05; Figure 4G).

We next investigated the mechanisms of Oxo-M mediated enhancement of DSE in the CeAL. One-way ANOVA revealed that 1±M Oxo-M-mediated DSE enhancement was attenuated in both $CB_1^{-/-}$ CeAL cells (Oxo-M-WT 57.16±2.56% vs. Oxo-M-$CB_1^{-/-}$ 87.03±3.77%, p<0.0001; Figure 4I and L) and CeAL cells pretreated with 10±M THL for at least 60 minutes (Oxo-M 57.16±2.56% vs. THL+ Oxo-M 86.08±2.73%, p<0.0001; Figure 4I and L). These results suggest that the simultaneous activation of mAChRs and postsynaptic depolarization results in the facilitation of 2-AG release at excitatory synapses within the CeAL. We next examined the muscarinic subtypes involved in the Oxo-M-mediated enhancement of depolarization-induced 2-AG release. Application of the M_1- or the M_3-preferring antagonists, 1 μ M pirenzepine or 500nM 4-DAMP respectively, significantly reduced the 1μM Oxo-M-dependent DSE enhancement (Oxo-M 57.16%±2.56% vs. Oxo-M +pirenzepine 73.92±3.92%, p<0.01; Oxo-M 57.16±2.56% vs. Oxo-M+4-DAMP 75.32±4.75%, p<0.01, Figure 4J–L). Collectively, these results suggest that both M_1 and M_3 receptors play a role in the mAChR-mediated enhancement of CeAL DSE. Interestingly, in $CB_1^{-/-}$ mice 10 second depolarization in the presence of Oxo-M elicited a small residual DSE (baseline 100.0±0.0% vs. 87.03±3.77%, p<0.01 by paired *t*-test), suggesting possible CB_1 independent residual effects induced by depolarization in the presence of Oxo-M.

Acute mAChR-driven eCB signaling in the CeAL

To determine whether acute application of Oxo-M can induce eCB release at CeAL glutamatergic synapses in the absence of depolarization, we applied Oxo-M for ~20 minutes and assessed eCB release during this period using pharmacological and genetic approaches (see Figure 5A for experimental design). Our results revealed that Oxo-M application dose-dependently suppressed eEPSC amplitude with maximal depression observed with 1±M Oxo-M (baseline 99.77±0.54% vs. Oxo-M 34.61±1.36%, p<0.0001 by paired *t*-test; Figures 5B–D and K). We next explored the contribution of CB_1 receptor activation to Oxo-M-mediated synaptic depression. Maximal Oxo-M-mediated depression was significantly attenuated in the presence of the CB_1 receptor antagonist SR141716 following either 0.3 μM Oxo-M (Oxo-M 46.24±4.25% vs. Oxo-M+SR141716 59.93±2.81%; t(8)=2.69, p<0.05) or 1 ±M Oxo-M application (Oxo-M 34.61±1.36% vs. Oxo-M+SR141716 53.11±2.73%; t(17)=5.98, p<0.001; See Figure 5CD and K).

We also examined the effects of SR141716 on Oxo-M induced elevation in PPR and found that SR141716 pretreatment significantly attenuated the 1±M Oxo-M-induced increase in PPR (p<0.0001; Figure 5E). Importantly, the residual Oxo-M depression in SR141716-treated slices was associated with a residual significant increase in PPR (p<0.001; Figure 5E), indicating that the non-CB_1 component of Oxo-M-induced depression is also

NIH-PA Author Manuscript

NIH-PA Author Manuscript

NIH-PA Author Manuscript

presynaptic in nature. Given that Oxo-M-induced synaptic depression is only partially CB_1-dependent, we sought to confirm these findings using $CB_1^{-/-}$ mice.Oxo-M induced synaptic depression was significantly attenuated in $CB_1^{-/-}$ mice (WT Oxo-M 37.91±2.83% vs. $CB_1^{-/-}$ Oxo-M 55.94±5.32%; t(12)=3.0, $p<0.05$; Figure 5F). The maximal 1μM Oxo-M-mediated increase in PPR was also significantly attenuated in $CB_1^{-/-}$ ($p<0.001$; Figure 5G). Collectively, these data indicate that Gq-receptor driven eCB mobilization can be initiated by mAChR activity in the CeAL, which in turn, contributes to Oxo-M-mediated synaptic depression of CeAL glutamatergic transmission.

Acute mAChR Activation Drives Ca^{2+}- and DAGL-*Independent* eCB Release

In light of previous studies, the roles of intracellular Ca^{2+} and DAGL in Gq-receptor driven eCB release remain uncertain (Edwards et al., 2006; Hashimotodani et al., 2005; Kim et al., 2002; Tanimura et al., 2010; Zhang et al., 2011). Therefore, we next examined the requirement for Ca^{2+} and DAGL activity in acute mAChR-driven eCB mobilization in the CeAL. First, we tested whether Oxo-M-mediated eCB release requires increases in intracellular Ca^{2+} concentrations $[Ca^{2+}]_i$. Postsynaptic loading of the fast Ca^{2+} chelator, BAPTA (20mM), did not affect 1μM Oxo-M-mediated synaptic depression and the maximal Oxo-M induced depression did not differ significantly from those observed under control conditions ($p>0.05$; Figure 5H and K). Similarly, THL pretreatment (10μM, ≥60 minutes) did not inhibit 1 μM Oxo-M-mediated depression of eEPSC amplitude ($p>0.05$; Figure 5I and K). Lastly, since recent studies have suggested phospholipase A2 (PLA2) may be required for 2-AG synaptic signaling in the cerebellum (Wang et al., 2012), we tested the involvement of PLA2 in Oxo-M-mediated synaptic depression as an alternate mechanism by which mAChR activation could release 2-AG. However, the PLA2 inhibitor, AACOCF3 (10μM), did not significantly affect Oxo-M-mediated synaptic depression ($p>0.05$; Figure 5J and K). These data suggest that acute mAChR-driven eCB release within the CeAL occurs independently of increases in $[Ca^{2+}]_i$ and does not require DAGL or PLA2 activity.

Prolonged mAChR Activation Drives Ca^{2+}- and DAGL-*Dependent* eCB Release

The lack of calcium and THL sensitivity of acute Oxo-M-mediated synaptic depression was somewhat surprising in light of recent studies implicating Ca^{2+} and DAGLα in Gq-receptor driven eCB release (Castillo et al., 2012; Hashimotodani et al., 2013; Katona and Freund, 2012). To exclude the possibility that the non-CB_1-dependent component of Oxo-M induced acute depression was potentially confounding our analysis, we took an alternate approach aimed at selectively evaluating CB_1-dependent synaptic effects of Oxo-M. To do this we pretreated slices with 1μM Oxo-M for ≥ 60 minutes and subsequently performed whole-cell patch clamp experiments where, after obtaining a stable baseline, we bath applied 5μM SR141716 in the continued presence of 1μM Oxo-M (see Figure 6A for experimental design). We reasoned that, if prolonged mAChR activation induces tonic eCB release and activation of CB_1 that subsequently depresses glutamatergic transmission, bath application of a CB_1 receptor antagonist should progressively relieve this tonic eCB inhibition and cause an apparent synaptic potentiation. Thus, this experimental design would allow us to isolate eCB-CB_1 mediated synaptic effects induced by prolonged mAChR activation. Consistent with this hypothesis, SR141716 (5μM) wash-on significantly increased eEPSC amplitude in slices pretreated with 1μM Oxo-M relative to control (no Oxo-M) conditions (Figure 6B–D). Maximal potentiation induced by SR141716 in the presence of continuous Oxo-M was 143.20±6.59% compared to 113.30±4.09% under control conditions ($p<0.001$; Figure 6B–D). Interestingly, unlike eCB release following brief Oxo-M application, continuous mAChR activation appeared to promote eCB mobilization through a THL- and a Ca^{2+}-*dependent* mechanism as pretreatment with 10μM THL or 20mM intracellular BAPTA completely abolished SR141716-induced synaptic potentiation ($p<0.0001$ for each condition; Figure 6C–E). Maximal SR141716-induced enhancement after 10μM THL

NIH-PA Author Manuscript

NIH-PA Author Manuscript

NIH-PA Author Manuscript

pretreatment (vehicle 113.30±4.09% vs. THL + Oxo-M 107.60±7.54%, p=0.88; Figure 6C–D) or 20mM BAPTA postsynaptic loading (vehicle 113.30±4.09% vs. BAPTA+ Oxo-M 99.25±6.10%, p=0.34; Figure 6C–D) was not significantly different from SR141716-induced synaptic potentiation under control (no Oxo-M) conditions. These data suggest a possible temporal switch from a BAPTA- and THL-*insensitive* to a BAPTA- and THL-*sensitive* mAChR-receptor-driven eCB release mechanism following prolonged mAChR stimulation.

Acute mAChR Activation Drives Synaptic AEA Release

Several recent studies have indicated that Gq-coupled receptors can mobilize AEA signaling (Chavez et al., 2010; Grueter et al., 2010). As such, we sought to investigate whether the Ca^{2+} and DAGL independent acute Oxo-M-mediated synaptic depression might be mediated via AEA, rather than 2-AG, signaling. To examine this possibility we determined the effects of inhibiting AEA degradation, with the fatty acid amide hydrolase (FAAH) inhibitor PF-3845, on Oxo-M-mediated acute synaptic depression (see Figure 7A for experimental design). PF-3845 (5μM) pretreatment attenuated Oxo-M-mediated synaptic depression at both 0.3μM ($p<0.01$) and 1 μM Oxo-M concentrations ($p<0.01$; Figure 7B–D). We also tested the effects of the monoacylglycerol lipase (MAGL) inhibitor, JZL-184 (2μM), on Oxo-M-induced synaptic depression to further rule out a role for 2-AG in acute Oxo-M-mediated synaptic depression. Consistent with the lack of BAPTA and THL sensitivity, prolonged MAGL blockade did not significantly affect subsequent Oxo-M-mediated acute synaptic depression at either 0.3 or 1μM Oxo-M concentration ($p>0.05$ for each; Figure 7B–D). Together these data indicate that inhibiting AEA, but not 2-AG, degradation modifies acute Oxo-M-mediated synaptic depression, however the direction of effect was somewhat unexpected. Specifically, if acute Oxo-M application causes release of AEA, blocking AEA degradation would be expected to increase Oxo-M synaptic depression rather than decrease it. The lack of enhancement was not due to a floor effect since both maximal and sub-maximal concentrations of Oxo-M showed reduced efficacy in the presence of FAAH, but not MAGL, inhibition.

An alternate explanation for our results is that PF-3845, but not JZL-184, occludes the effects of Oxo-M. If this were the case, PF-3845 would be expected to cause synaptic depression alone, which would then occlude subsequent AEA-mediated synaptic depression initiated by acute Oxo-M application. Consistent with this hypothesis, 5μM PF-3845 wash-on produced a CB_1-dependent synaptic depression of glutamatergic transmission (PF-3845+vehicle 83.31%±5.34% vs. PF-3845+SR141716 102.80%±3.91%; $t(14)=2.79$, $p<0.05$; Figure 7E–F). These data, combined with the lack of occlusion of acute Oxo-M-mediated synaptic depression by the MAGL inhibitor JZL-184 strongly implicate AEA, rather than 2-AG, as the eCB ligand subserving synaptic depression induced by acute Oxo-M application. However, it is possible the lack of occlusion by MAGL inhibition could be due to the fact that JZL-184 alone did not produce synaptic depression. To exclude this possibility and strengthen the support for an AEA-mediated process, we tested the ability of JZL-184 to cause synaptic depression of glutamatergic transmission. Consistent with our hypothesis, JZL-184 produced a CB_1 dependent synaptic depression of glutamatergic signaling (JZL-184+ vehicle 74.29%±4.24% vs. JZL-184+SR141716 96.38%±2.97%; $t(9)=4.1$, $p< 0.01$; Figure 7G–H). Taken together, these data provide converging evidence that acute Oxo-M-mediated synaptic depression causes synthesis/release of AEA that acts on CB_1 receptors to reduce glutamate release, and that prolonged Oxo-M stimulation of mAChRs enhances DSE and causes tonic CB_1-mediated synaptic depression via release of 2-AG through the canonical calcium-DAGL-dependent pathway (Figure 7I–J).

NIH-PA Author Manuscript

NIH-PA Author Manuscript

NIH-PA Author Manuscript

Lack of Oxo-M-Mediated Acute or Tonic eCB Signaling in Striatum

Thus far, our data indicate that acute Oxo-M activation of mAChRs drives AEA release and subsequent depression of glutamatergic signaling via CB_1 activation. In contrast, prolonged mAChR activity results in 2-AG-mediated tonic CB_1 activation and enhancement of DSE. Since this is the first demonstration, to the best of our knowledge, of temporally dissociated AEA and 2-AG release by the same stimulus, we wanted to examine whether this was a generalizable phenomenon. Therefore, we tested this phenomenon in the striatum given the strong morphological, hodological, and cytoarchitectural similarities between the striatum and the CeAL (McDonald, 1982). Acute application of Oxo-M (1μM) caused robust presynaptic depression in the striatum, however, this depression was not affected by SR141716 pretreatment ($p>0.05$; Figure S3 A–C). Similarly, SR141716 failed to produce synaptic potentiation in the presence or absence of prolonged Oxo-M (1μM) pre-treatment (Figure S3D). In contrast, prolonged Oxo-M (1μM) application was able to enhance DSE relative to control conditions ($p<0.01$; Figure S3E) and this enhancement was blocked by SR141716 ($p<0.0001$). These data indicate that Oxo-M (1μM) is able to enhance DSE in the striatum, but that mAChRs do not trigger acute AEA or tonic 2-AG release to regulate glutamatergic transmission in this region. Thus, mAChR-driven multimodal eCB release may not be a generalized feature of central synapses.

DISCUSSION

eCB Signaling at CeAL Glutamatergic Synapses

Here we report the distribution and subcellular localization of CB_1 receptors and the 2-AG synthetic enzyme, DAGLα, in the CeAL. In contrast to earlier studies, where CB_1 receptor expression was below detection threshold in the CeAL (Katona et al., 2001), here we utilized a high-affinity CB_1 receptor antibody to conclusively demonstrate the presence of CB_1 receptor protein in the CeAL (see (Katona et al., 2006; Uchigashima et al., 2007)). High-resolution analyses showed CB_1 receptors localized to presynaptic terminals forming asymmetric synapses onto postsynaptic dendrites and dendritic spines. In contrast, DAGLα was observed in the CeAL at both the mRNA and protein level, with ultrastructural studies demonstrating clear localization within postsynaptic dendritic spine heads and dendritic shafts adjacent to asymmetric synapses. Overall, these data support the well-established anatomical substrate for retrograde eCB signaling at central synapses (Katona and Freund, 2012).

Consistent with our anatomical data, we found that activation of CB_1 receptors reliably reduced eEPSC amplitude, while effects on GABAergic transmission were more variable (Katona et al., 2001). Interestingly, the cannabinoid agonist CP55940 reduced eEPSC amplitude without clear effect on PPR. In contrast, 2-AG-ether and DSE both cause synaptic depression associated with an increase in PPR. Although our data that CP55940 affected the frequency, but not amplitude, of sEPSCs suggest a presynaptic site of action, the lack of effect on PPR was unexpected and inconsistent with the effects of DSE and 2-AG-ether. Although previous studies have shown presynaptic inhibition of glutamate release in the CeAL by a decrease the number of release sites rather than release probability (Delaney et al., 2007), the mechanistic discrepancy between different CB_1 ligands is more difficult to explain. One possibility could be related to ligand-directed signaling at the CB_1 receptor (Hudson et al., 2010), which would imply multiple presynaptic mechanisms downstream of CB_1 receptor activation could result in reduced glutamatergic transmission.

Multiple Modes of Postsynaptic eCB Mobilization by CeAL Neurons

Consistent with our studies demonstrating eCB signaling elements at CeAL excitatory synapses and CB_1 receptor-mediated depression of glutamatergic signaling, we found that

NIH-PA Author Manuscript

NIH-PA Author Manuscript

NIH-PA Author Manuscript

CeAL neurons express prototypic 2-AG-mediated eCB signaling, i.e. DSE, mediated via a calcium-dependent, THL-sensitive, and CB_1-dependent mechanism. These studies add to a recent demonstration of DSE in the CeAM (Kamprath et al., 2011), and tonic eCB release at CeAM GABAergic synapses (Roberto et al., 2010). We next examined the mechanisms by which Gq-coupled mAChRs initiate eCB signaling at CeAL glutamatergic synapses. Our data indicate that acute application of Oxo-M causes a robust presynaptic depression that is partially mediated via activation of CB_1 receptors, consistent with findings in the periaqueductal grey (Lau and Vaughan, 2008). Mechanistically, this acute CB_1-dependent depression does not require elevations in intracellular calcium, is THL-*insensitive*, and does not require PLA2 activity. Moreover, inhibition of 2-AG degradation with JZL-184 did not affect Oxo-M-mediated acute synaptic depression. Taken together, these data appear to exclude 2-AG as the eCB ligand mediating the acute CB_1-dependent synaptic depression induced by short-term mAChR activation.

We next tested the hypothesis that another eCB ligand, namely AEA, mediates eCB-mediated synaptic depression induced by acute mAChR activation. We found that FAAH inhibition, which on its own caused a CB_1-dependent synaptic depression of glutamatergic transmission, partially occluded acute Oxo-M-mediated synaptic depression, implicating AEA in this process. Huang and Woolley (2012), who showed that estrogen-induced depression of GABAergic transmission in the hippocampus was occluded by FAAH inhibition, but not MAGL inhibition, reached similar conclusions in their system (Huang and Woolley, 2012). However, clear delineation of the biosynthetic pathway for synaptic AEA synthesis and the development of pharmacological tools to probe this system will be required to conclusively assign AEA as the eCB ligand mediating acute Oxo-M driven synaptic depression.

In contrast to the putative AEA-mediated synaptic depression induced by acute mAChR activation, prolonged activation of mAChR increases 2-AG-mediated signaling processes. First, after prolonged Oxo-M incubation, DSE is enhanced in an $M_{1/3}$-dependent, THL-sensitive, and CB_1-dependent manner which is consistent with findings in other brain regions (Kano et al., 2009). Interestingly, our SR141716 wash-on studies revealed strong synaptic potentiation by CB_1 blockade in slices incubated with Oxo-M, but not vehicle. These data suggest tonic eCB release can be induced by prolonged mAChR activity. This synaptic potentiation required intracellular calcium and was THL-*sensitive*, strongly suggesting that this Oxo-M-induced tonic eCB signal is mediated by 2-AG synthesized by the canonical calcium-DAGL-dependent pathway (Kano et al., 2009). These findings are consistent with recent studies in MAGL knock-out mice, which suggest that 2-AG can act as a tonic eCB retrograde messenger (Pan et al., 2011). Overall, these data indicate that CeAL neurons can mobilize multiple forms of eCB signaling to modulate afferent glutamatergic transmission.

Functional Implications of Temporally Dissociated Multimodal eCB Signaling

Previous studies have demonstrated that some cells can produce both AEA and 2-AG that act as retrograde eCBs signals (Huang and Woolley, 2012; Kim and Alger, 2010; Lerner and Kreitzer, 2012; Mathur et al., 2013; Puente et al., 2011). Similarly, several studies have demonstrated that activation of Gq-coupled receptors can induce 2-AG and also AEA release in several brain regions (Chavez et al., 2010; Grueter et al., 2010; Hashimotodani et al., 2013; Lerner and Kreitzer, 2012; Maccarrone et al., 2008). However, to the best of our knowledge, our data are the first to provide experimental evidence that AEA and 2-AG can be released in response to activation of the same Gq-coupled receptor depending only on the duration of Gq-receptor stimulation. Specifically, acute mAChR activation causes short-lived AEA-mediated synaptic depression, while prolonged mAChR stimulation causes 2-

NIH-PA Author Manuscript

NIH-PA Author Manuscript

NIH-PA Author Manuscript

AG-mediated tonic eCB depression of glutamatergic transmission. Thus, in CeAL neurons, mAChR stimulation can initiate multimodal eCB signaling depending only on the duration of Gq-receptor stimulation. The mechanistic basis for this temporal "switch" remains to be determined, but is likely related to temporal differences in the coupling of mAChRs to distinct signaling pathways important for AEA and 2-AG synthesis (Mangoura et al., 1995; McKenzie et al., 1992; Schmidt et al., 1995).

Recent studies have begun to highlight the dissociable roles of AEA and 2-AG signaling on multiple levels. For example, in the bed nucleus of the stria terminalis, AEA mediates long-term synaptic depression, while 2-AG mediates short-term synaptic depression (STD) in the form of DSE (Puente et al., 2011). In contrast, in the striatum different forms of associative neural activity can elicit both AEA- and 2-AG-mediated long-term depression (Lerner and Kreitzer, 2012). More recently, different inhibitory synapses in the striatum have been shown to release AEA and 2-AG in a state-dependent manner (Mathur et al., 2013). Thus, AEA and 2-AG are clearly not "redundant" signaling molecules and have distinct duration-, activity-, and synapse-dependent effects. Here we add to this eCB signaling diversity by demonstrating temporally-dissociated mobilization of AEA and 2-AG signaling in response to mAChR activity. Continued investigation of multimodal eCB signaling could provide insight into the activity-dependent mechanisms sculpting synaptic efficacy.

Here we show that eCB signaling suppresses afferent glutamatergic transmission onto CeAL neurons, which could represent an important synaptic mechanism regulating stress response physiology and anxiety-like behaviors. Specifically, inhibition of excitatory drive to protein kinase C-δ-expressing GABAergic CeAL projection neurons would disinhibit CeAM neurons and increase fear and anxiety responses (Haubensak et al., 2010). This model is consistent with well-known anxiogenic effects of high doses of exogenous cannabinoids (Patel and Hillard, 2006), and therefore could represent a synaptic correlate of cannabinoid anxiogenesis. In contrast, inhibition of glutamatergic drive to locally-targeting somatostatin-expressing GABAergic neurons would disinhibit CeAL projection neurons and, in turn, inhibit CeAM activity thereby reducing anxiety and fear responses, which is the primary physiological function of eCB signaling (Hill et al., 2009; Lutz, 2007; Riebe et al., 2012). Future studies aimed at elucidating the afferent-and cell type-specific effects of eCB signaling within the CeA microcircuitry will be critical to advancing our understanding of the synaptic mechanisms by which eCB signaling modulates stress-responses, anxiety, and emotional learning.

EXPERIMENTAL PROCEDURES

Anatomical Experiments

In situ hybridization, immunoperoxidase, and immuno-electron microscopy experiments were conducted as previously described (Peterfi et al., 2012), and detailed in the supplementary information. Briefly, we prepared antisense and sense riboprobes against a 1170 base pair (bp) long section (from position 1967 to 3136 in the open reading frame) of mouse DAGLα coding sequence using the following primers: forward, 5'-TCA TGG AGG GGC TCA ATA AG; reverse, 5'-CTA GCG TGC CGA GAT GAC CA (Katona et al., 2006). The CB_1 riboprobe was generated against a 738 bp long region of mouse CB_1 coding sequence (from position 548 to 1285 in the open reading frame; forward primer, 5'-CTA ATC AAA GAC TGA GGT TA; reverse primer, 5'- CAC AGA GCC TCG GCA GAC GT). Free-floating immunoperoxidase staining also followed the previously established protocol (Peterfi et al., 2012). For electron microscopic analyses, after development of the immunostaining, the sections were treated with 0.5% OsO_4, dehydrated in an ascending series of ethanol and acetonitrile solutions, and finally embedded into Durcupan™ ACM Fluka (Sigma). During dehydration, sections were also treated with 1% uranyl acetate in

NIH-PA Author Manuscript

NIH-PA Author Manuscript

NIH-PA Author Manuscript

70% ethanol for 20 minutes. After overnight incubation in Durcupan, the sections were mounted onto glass slides and coverslips were sealed by polymerization of Durcupan at 56 °C for 48 hours. From sections embedded in Durcupan, areas of interest from the CeAL were re-embedded and re-sectioned for electron microscopy.

Electrophysiology

Whole-cell voltage clamp and field potential electrophysiological experiments were carried out in 4–5 week old male ICR mice as described previously (Patel et al., 2009; Sumislawski et al., 2011). Briefly, Mice were anesthetized with isoflurane and transcardially perfused with ice-cold high sucrose, low Na^+-containing ACSF. Following decapitation, the brain was removed and a 3mm coronal block of the amygdala was cut using an ice-chilled, coronal brain matrix. Thereafter, coronal slices (200–300μm) were made using a Leica VT1000S vibratome (Leica Microsystems, Bannockburn, IL) in a 1–4°C oxygenated (95% v/v O_2, 5% v/v CO_2) ACSF comprised of (in mM): 208 sucrose, 2.5 KCl, 1.6 NaH_2PO_4, 1 $CaCl_2{\cdot}2H_2O$, 4 $MgCl_2{\cdot}6H_2O$, 4 $MgSO_4{\cdot}7H_2O$, 26 $NaHCO_3$, 1 ascorbate, 3 Na-pyruvate, and 20 glucose. Whole-cell voltage-clamp recordings were performed on CeAL neurons easily identified visually by their medium-sized, spherical somata. Patch electrodes were pulled on a Flaming/Brown microelectrode puller (Sutter Instruments) and filled with solution containing (in mM): 120 K^+-gluconate, 4 NaCl, 10 HEPES, 20 KCl, 4 Mg-ATP, 0.3 Na-GTP, and 10 Na-phosphocreatine (pH 7.25–7.35, adjusted with KOH). eEPSCs were recorded from CeAL neurons via local microstimulation, ~100μm from the cell soma. Experimental details are described in the supplemental materials.

Statistical Analysis

Statistical significance between the means of two independent groups was assessed using two-tailed paired or unpaired *t*-test unless variance differed significantly (Bartlett's test for equal variances), in which case non-parametric Mann-Whitney (U) tests were used. Statistical comparisons between two or more groups were performed using one or two-way analysis of variance (ANOVA). F and P values for ANOVA are provided above individual figures. Post hoc analyses were conducted by Dunnett's or Sidak's test as indicated in the text.

Supplementary Material

Refer to Web version on PubMed Central for supplementary material.

Acknowledgments

These studies were supported by NIH Grants MH090412 and MH100096 (S.P.), DA011322 and DA021696 (K.M.), the Momentum Program of the Hungarian Academy of Sciences (LP2013-54), and by the European Research Council Grant 243153 (I.K.). I.K. is the recipient of a Wellcome Trust International Senior Research Fellowship. The authors are also indebted to Erika Tischler and Balázs Pintér for their excellent technical assistance. The authors also wish to thank Mr. László Barna, the Nikon Microscopy Center at IEM.

REFERENCES

Amano T, Unal CT, Pare D. Synaptic correlates of fear extinction in the amygdala. Nat. Neurosci. 2010; 13:489–494. [PubMed: 20208529]

Cassell MD, Freedman LJ, Shi C. The intrinsic organization of the central extended amygdala. Ann. N Y Acad. Sci. 1999; 877:217–241. [PubMed: 10415652]

Castillo PE, Younts TJ, Chavez AE, Hashimotodani Y. Endocannabinoid signaling and synaptic function. Neuron. 2012; 76:70–81. [PubMed: 23040807]

NIH-PA Author Manuscript

NIH-PA Author Manuscript

NIH-PA Author Manuscript

Chavez AE, Chiu CQ, Castillo PE. TRPV1 activation by endogenous anandamide triggers postsynaptic long-term depression in dentate gyrus. Nat. Neurosci. 2010; 13:1511–1518. [PubMed: 21076423]

Ciocchi S, Herry C, Grenier F, Wolff SB, Letzkus JJ, Vlachos I, Ehrlich I, Sprengel R, Deisseroth K, Stadler MB, et al. Encoding of conditioned fear in central amygdala inhibitory circuits. Nature. 2010; 468:277–282. [PubMed: 21068837]

Cravatt BF, Demarest K, Patricelli MP, Bracey MH, Giang DK, Martin BR, Lichtman AH. Supersensitivity to anandamide and enhanced endogenous cannabinoid signaling in mice lacking fatty acid amide hydrolase. Proc. Natl. Acad. Sci. U S A. 2001; 98:9371–9376. [PubMed: 11470906]

Davis M. Neurobiology of fear responses: the role of the amygdala. J. Neuropsychiatry. Clin. Neurosci. 1997; 9:382–402. [PubMed: 9276841]

Delaney AJ, Crane JW, Sah P. Noradrenaline modulates transmission at a central synapse by a presynaptic mechanism. Neuron. 2007; 56:880–892. [PubMed: 18054863]

Dinh TP, Carpenter D, Leslie FM, Freund TF, Katona I, Sensi SL, Kathuria S, Piomelli D. Brain monoglyceride lipase participating in endocannabinoid inactivation. Proc. Natl. Acad. Sci. U S A. 2002; 99:10819–10824. [PubMed: 12136125]

Dong YL, Fukazawa Y, Wang W, Kamasawa N, Shigemoto R. Differential postsynaptic compartments in the laterocapsular division of the central nucleus of amygdala for afferents from the parabrachial nucleus and the basolateral nucleus in the rat. J. Comp. Neurol. 2010; 518:4771–4791. [PubMed: 20963828]

Edwards DA, Kim J, Alger BE. Multiple mechanisms of endocannabinoid response initiation in hippocampus. J Neurophysiol. 2006; 95:67–75. [PubMed: 16207781]

Ehrlich I, Humeau Y, Grenier F, Ciocchi S, Herry C, Luthi A. Amygdala inhibitory circuits and the control of fear memory. Neuron. 2009; 62:757–771. [PubMed: 19555645]

El-Amamy H, Holland PC. Dissociable effects of disconnecting amygdala central nucleus from the ventral tegmental area or substantia nigra on learned orienting and incentive motivation. Eur. J. Neurosci. 2007; 25:1557–1567. [PubMed: 17425582]

Groshek F, Kerfoot E, McKenna V, Polackwich AS, Gallagher M, Holland PC. Amygdala central nucleus function is necessary for learning, but not expression, of conditioned auditory orienting. Behav. Neurosci. 2005; 119:202–212. [PubMed: 15727525]

Grueter BA, Brasnjo G, Malenka RC. Postsynaptic TRPV1 triggers cell type-specific long-term depression in the nucleus accumbens. Nat. Neurosci. 2010; 13:1519–1525. [PubMed: 21076424]

Hanus L, Abu-Lafi S, Fride E, Breuer A, Vogel Z, Shalev DE, Kustanovich I, Mechoulam R. 2-arachidonyl glyceryl ether, an endogenous agonist of the cannabinoid CB1 receptor. Proc. Natl. Acad. Sci. U S A. 2001; 98:3662–3665. [PubMed: 11259648]

Hashimotodani Y, Ohno-Shosaku T, Kano M. Ca(2+)-assisted receptor-driven endocannabinoid release: mechanisms that associate presynaptic and postsynaptic activities. Curr. Opin. Neurobiol. 2007; 17:360–365. [PubMed: 17419048]

Hashimotodani Y, Ohno-Shosaku T, Tanimura A, Kita Y, Sano Y, Shimizu T, Di Marzo V, Kano M. Acute inhibition of diacylglycerol lipase blocks endocannabinoid-mediated retrograde signalling: evidence for on-demand biosynthesis of 2-arachidonoylglycerol. J. Physiol. 2013; 591:4765–4776. [PubMed: 23858009]

Hashimotodani Y, Ohno-Shosaku T, Tsubokawa H, Ogata H, Emoto K, Maejima T, Araishi K, Shin HS, Kano M. Phospholipase Cbeta serves as a coincidence detector through its Ca2+ dependency for triggering retrograde endocannabinoid signal. Neuron. 2005; 45:257–268. [PubMed: 15664177]

Haubensak W, Kunwar PS, Cai H, Ciocchi S, Wall NR, Ponnusamy R, Biag J, Dong HW, Deisseroth K, Callaway EM, et al. Genetic dissection of an amygdala microcircuit that gates conditioned fear. Nature. 2010; 468:270–276. [PubMed: 21068836]

Hill MN, Hillard CJ, Bambico FR, Patel S, Gorzalka BB, Gobbi G. The therapeutic potential of the endocannabinoid system for the development of a novel class of antidepressants. Trends. Pharmacol. Sci. 2009; 30:484–493. [PubMed: 19732971]

NIH-PA Author Manuscript

NIH-PA Author Manuscript

NIH-PA Author Manuscript

Hill MN, Patel S, Campolongo P, Tasker JG, Wotjak CT, Bains JS. Functional interactions between stress and the endocannabinoid system: from synaptic signaling to behavioral output. J. Neurosci. 2010; 30:14980–14986. [PubMed: 21068301]

Huang GZ, Woolley CS. Estradiol acutely suppresses inhibition in the hippocampus through a sex-specific endocannabinoid and mGluR-dependent mechanism. Neuron. 2012; 74:801–808. [PubMed: 22681685]

Hudson BD, Hebert TE, Kelly ME. Ligand- and heterodimer-directed signaling of the CB(1) cannabinoid receptor. Mol. Pharmacol. 2010; 77:1–9. [PubMed: 19837905]

Kamprath K, Romo-Parra H, Haring M, Gaburro S, Doengi M, Lutz B, Pape HC. Short-term adaptation of conditioned fear responses through endocannabinoid signaling in the central amygdala. Neuropsychopharmacology. 2011; 36:652–663. [PubMed: 20980994]

Kano M, Ohno-Shosaku T, Hashimotodani Y, Uchigashima M, Watanabe M. Endocannabinoid-mediated control of synaptic transmission. Physiol. Rev. 2009; 89:309–380. [PubMed: 19126760]

Katona I, Freund TF. Multiple functions of endocannabinoid signaling in the brain. Annu. Rev. Neurosci. 2012; 35:529–558. [PubMed: 22524785]

Katona I, Rancz EA, Acsady L, Ledent C, Mackie K, Hajos N, Freund TF. Distribution of CB1 cannabinoid receptors in the amygdala and their role in the control of GABAergic transmission. J. Neurosci. 2001; 21:9506–9518. [PubMed: 11717385]

Katona I, Urban GM, Wallace M, Ledent C, Jung KM, Piomelli D, Mackie K, Freund TF. Molecular composition of the endocannabinoid system at glutamatergic synapses. J. Neurosci. 2006; 26:5628–5637. [PubMed: 16723519]

Kim J, Alger BE. Reduction in endocannabinoid tone is a homeostatic mechanism for specific inhibitory synapses. Nat. Neurosci. 2010; 13:592–600. [PubMed: 20348918]

Kim J, Isokawa M, Ledent C, Alger BE. Activation of muscarinic acetylcholine receptors enhances the release of endogenous cannabinoids in the hippocampus. J. Neurosci. 2002; 22:10182–10191. [PubMed: 12451119]

Lau BK, Vaughan CW. Muscarinic modulation of synaptic transmission via endocannabinoid signalling in the rat midbrain periaqueductal gray. Mol. Pharmacol. 2008; 74:1392–1398. [PubMed: 18678620]

Lerner TN, Kreitzer AC. RGS4 is required for dopaminergic control of striatal LTD and susceptibility to parkinsonian motor deficits. Neuron. 2012; 73:347–359. [PubMed: 22284188]

Li H, Penzo MA, Taniguchi H, Kopec CD, Huang ZJ, Li B. Experience-dependent modification of a central amygdala fear circuit. Nat. Neurosci. 2013; 16:332–339. [PubMed: 23354330]

Li S, Kirouac GJ. Projections from the paraventricular nucleus of the thalamus to the forebrain, with special emphasis on the extended amygdala. J. Comp. Neurol. 2008; 506:263–287. [PubMed: 18022956]

Long JZ, Li W, Booker L, Burston JJ, Kinsey SG, Schlosburg JE, Pavon FJ, Serrano AM, Selley DE, Parsons LH, et al. Selective blockade of 2-arachidonoylglycerol hydrolysis produces cannabinoid behavioral effects. Nat Chem Biol. 2009; 5:37–44. [PubMed: 19029917]

Ludanyi A, Hu SS, Yamazaki M, Tanimura A, Piomelli D, Watanabe M, Kano M, Sakimura K, Magloczky Z, Mackie K, et al. Complementary synaptic distribution of enzymes responsible for synthesis and inactivation of the endocannabinoid 2-arachidonoylglycerol in the human hippocampus. Neuroscience. 2011; 174:50–63. [PubMed: 21035522]

Lutz B. The endocannabinoid system and extinction learning. Mol. Neurobiol. 2007; 36:92–101. [PubMed: 17952654]

Maccarrone M, Rossi S, Bari M, De Chiara V, Fezza F, Musella A, Gasperi V, Prosperetti C, Bernardi G, Finazzi-Agro A, et al. Anandamide inhibits metabolism and physiological actions of 2-arachidonoylglycerol in the striatum. Nat. Neurosci. 2008; 11:152–159. [PubMed: 18204441]

Mangoura D, Sogos V, Pelletiere C, Dawson G. Differential regulation of phospholipases C and D by phorbol esters and the physiological activators carbachol and glutamate in astrocytes from chicken embryo cerebrum and cerebellum. Brain Res. Dev. Brain Res. 1995; 87:12–21.

Mathur BN, Tanahira C, Tamamaki N, Lovinger DM. Voltage drives diverse endocannabinoid signals to mediate striatal microcircuit-specific plasticity. Nat. Neurosci. 2013; 16:1275–1283. [PubMed: 23892554]

NIH-PA Author Manuscript

NIH-PA Author Manuscript

NIH-PA Author Manuscript

McDonald AJ. Cytoarchitecture of the central amygdaloid nucleus of the rat. J. Comp. Neurol. 1982; 208:401–418. [PubMed: 7119168]

McDonald AJ, Shammah-Lagnado SJ, Shi C, Davis M. Cortical afferents to the extended amygdala. Ann. N Y Acad. Sci. 1999; 877:309–338.

McKenzie FR, Seuwen K, Pouyssegur J. Stimulation of phosphatidylcholine breakdown by thrombin and carbachol but not by tyrosine kinase receptor ligands in cells transfected with M1 muscarinic receptors. Rapid desensitization of phosphocholine-specific (PC) phospholipase D but sustained activity of PC-phospholipase C. J. Biol. Chem. 1992; 267:22759–22769. [PubMed: 1331066]

Narushima M, Hashimoto K, Kano M. Endocannabinoid-mediated short-term suppression of excitatory synaptic transmission to medium spiny neurons in the striatum. Neurosci. Res. 2006; 54:159–164. [PubMed: 16413076]

Ohno-Shosaku T, Hashimotodani Y, Maejima T, Kano M. Calcium signaling and synaptic modulation: regulation of endocannabinoid-mediated synaptic modulation by calcium. Cell Calcium. 2005; 38:369–374. [PubMed: 16085309]

Ohno-Shosaku T, Tanimura A, Hashimotodani Y, Kano M. Endocannabinoids and retrograde modulation of synaptic transmission. Neuroscientist. 2012; 18:119–132. [PubMed: 21531987]

Pan B, Wang W, Zhong P, Blankman JL, Cravatt BF, Liu QS. Alterations of endocannabinoid signaling, synaptic plasticity, learning, and memory in monoacylglycerol lipase knock-out mice. J. Neurosci. 2011; 31:13420–13430. [PubMed: 21940435]

Pape HC, Pare D. Plastic synaptic networks of the amygdala for the acquisition, expression, and extinction of conditioned fear. Physiol. Rev. 2010; 90:419–463. [PubMed: 20393190]

Patel S, Hillard CJ. Pharmacological evaluation of cannabinoid receptor ligands in a mouse model of anxiety: further evidence for an anxiolytic role for endogenous cannabinoid signaling. J. Pharmacol. Exp. Ther. 2006; 318:304–311. [PubMed: 16569753]

Patel S, Kingsley PJ, Mackie K, Marnett LJ, Winder DG. Repeated homotypic stress elevates 2-arachidonoylglycerol levels and enhances short-term endocannabinoid signaling at inhibitory synapses in basolateral amygdala. Neuropsychopharmacology. 2009; 34:2699–2709. [PubMed: 19675536]

Peterfi Z, Urban GM, Papp OI, Nemeth B, Monyer H, Szabo G, Erdelyi F, Mackie K, Freund TF, Hajos N, Katona I. Endocannabinoid-mediated long-term depression of afferent excitatory synapses in hippocampal pyramidal cells and GABAergic interneurons. J. Neurosci. 2012; 32:14448–14463. [PubMed: 23055515]

Puente N, Cui Y, Lassalle O, Lafourcade M, Georges F, Venance L, Grandes P, Manzoni OJ. Polymodal activation of the endocannabinoid system in the extended amygdala. Nat. Neurosci. 2011; 14:1542–1547. [PubMed: 22057189]

Ramikie TS, Patel S. Endocannabinoid signaling in the amygdala: anatomy, synaptic signaling, behavior, and adaptations to stress. Neuroscience. 2011; 204:38–52. [PubMed: 21884761]

Riebe CJ, Pamplona FA, Kamprath K, Wotjak CT. Fear relief-toward a new conceptual frame work and what endocannabinoids gotta do with it. Neuroscience. 2012; 204:159–185. [PubMed: 22173015]

Roberto M, Cruz M, Bajo M, Siggins GR, Parsons LH, Schweitzer P. The endocannabinoid system tonically regulates inhibitory transmission and depresses the effect of ethanol in central amygdala. Neuropsychopharmacology. 2010; 35:1962–1972. [PubMed: 20463657]

Roozendaal B, van der Zee EA, Hensbroek RA, Maat H, Luiten PG, Koolhaas JM, Bohus B. Muscarinic acetylcholine receptor immunoreactivity in the amygdala--II. Fear-induced plasticity. Neuroscience. 1997; 76:75–83.

Schmidt M, Fasselt B, Rumenapp U, Bienek C, Wieland T, van Koppen CJ, Jakobs KH. Rapid and persistent desensitization of m3 muscarinic acetylcholine receptor-stimulated phospholipase D. Concomitant sensitization of phospholipase C. J. Biol. Chem. 1995; 270:19949–19956. [PubMed: 7650010]

Straiker A, Mackie K. Metabotropic suppression of excitation in murine autaptic hippocampal neurons. J. Physiol. 2007; 578:773–785. [PubMed: 17110416]

Sumislawski JJ, Ramikie TS, Patel S. Reversible gating of endocannabinoid plasticity in the amygdala by chronic stress: a potential role for monoacylglycerol lipase inhibition in the prevention of

NIH-PA Author Manuscript

NIH-PA Author Manuscript

NIH-PA Author Manuscript

stress-induced behavioral adaptation. Neuropsychopharmacology. 2011; 36:2750–2761. [PubMed: 21849983]

Sun N, Yi H, Cassell MD. Evidence for a GABAergic interface between cortical afferents and brainstem projection neurons in the rat central extended amygdala. J. Comp. Neurol. 1994; 340:43–64. [PubMed: 7513719]

Tanimura A, Yamazaki M, Hashimotodani Y, Uchigashima M, Kawata S, Abe M, Kita Y, Hashimoto K, Shimizu T, Watanabe M, et al. The endocannabinoid 2-arachidonoylglycerol produced by diacylglycerol lipase alpha mediates retrograde suppression of synaptic transmission. Neuron. 2010; 65:320–327. [PubMed: 20159446]

Tye KM, Prakash R, Kim SY, Fenno LE, Grosenick L, Zarabi H, Thompson KR, Gradinaru V, Ramakrishnan C, Deisseroth K. Amygdala circuitry mediating reversible and bidirectional control of anxiety. Nature. 2011; 471:358–362. [PubMed: 21389985]

Uchigashima M, Narushima M, Fukaya M, Katona I, Kano M, Watanabe M. Subcellular arrangement of molecules for 2-arachidonoyl-glycerol-mediated retrograde signaling and its physiological contribution to synaptic modulation in the striatum. J. Neurosci. 2007; 27:3663–3676. [PubMed: 17409230]

van der Zee EA, Roozendaal B, Bohus B, Koolhaas JM, Luiten PG. Muscarinic acetylcholine receptor immunoreactivity in the amygdala--I. Cellular distribution correlated with fear-induced behavior. Neuroscience. 1997; 76:63–73. [PubMed: 8971759]

Wang DJ, Yang D, Su LD, Xie YJ, Zhou L, Sun CL, Wang Y, Wang XX, Zhou L, Shen Y. Cytosolic phospholipase A2 alpha/arachidonic acid signaling mediates depolarization-induced suppression of excitation in the cerebellum. PLoS ONE. 2012; 7:e41499. [PubMed: 22927908]

Yoshida T, Uchigashima M, Yamasaki M, Katona I, Yamazaki M, Sakimura K, Kano M, Yoshioka M, Watanabe M. Unique inhibitory synapse with particularly rich endocannabinoid signaling machinery on pyramidal neurons in basal amygdaloid nucleus. Proc. Natl. Acad. Sci. U S A. 2011; 108:3059–3064. [PubMed: 21282604]

Zhang L, Wang M, Bisogno T, Di Marzo V, Alger BE. Endocannabinoids generated by Ca2+ or by metabotropic glutamate receptors appear to arise from different pools of diacylglycerol lipase. PLoS ONE. 2011; 6:e16305. [PubMed: 21305054]

NIH-PA Author Manuscript

NIH-PA Author Manuscript

NIH-PA Author Manuscript

HIGHLIGHTS

1) eCB signaling components are expressed at CeA glutamatergic synapses.

2) Activation of the CB_1 receptor suppresses glutamate release in the CeA.

3) CeA neurons express calcium- and Gq-receptor-driven eCB signaling.

4) CeA muscarinic receptors drive temporally-distinct multimodal eCB release.

NIH-PA Author Manuscript

NIH-PA Author Manuscript

NIH-PA Author Manuscript

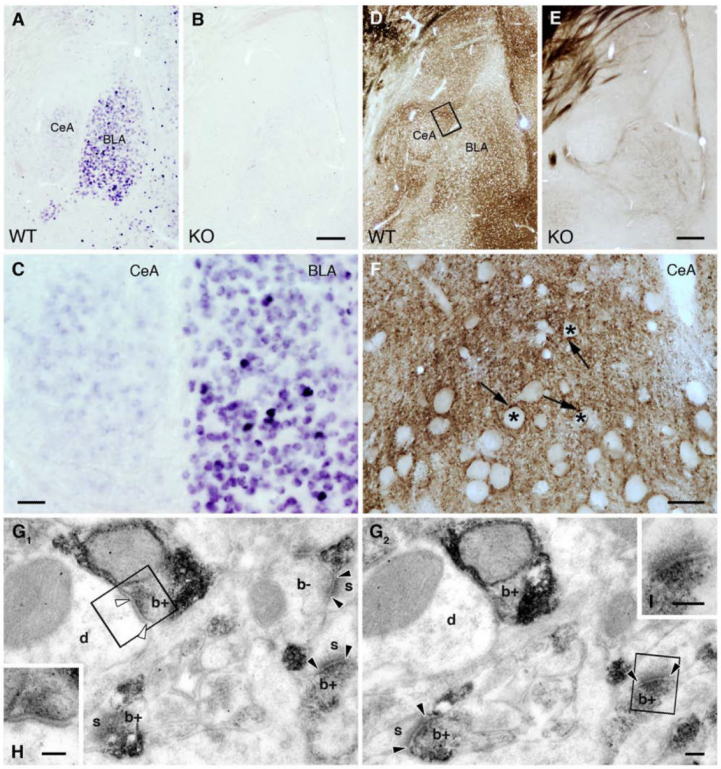

Figure 1. CB_1 Receptors are Present on Excitatory Terminals in the CeAL

(A) *In situ* hybridization reveals the presence of CB_1 mRNA in both the CeA and the BLA of wild type mice. (B) The specificity of the riboprobe is confirmed by using $CB_1^{-/-}$ animals. (C) The very high levels of CB_1 mRNA observed in a few scattered neurons in the BLA likely correspond to GABAergic interneurons. The vast majority of BLA neurons express moderate levels of CB_1 mRNA. In contrast, CB_1 mRNA expression in the CeA was only slightly above detection threshold. (D–E) Immunoperoxidase staining demonstrates the presence of the CB_1 protein in both the CeA and BLA, which was confirmed in our $CB_1^{-/-}$ samples. (F) Higher magnification light micrographs reveal the dense CB_1 labeling in the neuropil throughout the CeAL. Asterisks depict CB_1-immunonegative cell bodies, whereas CB_1-immunopositive labeling appears as punctate staining indicating the compartmentalized distribution of the protein. (G_1-G_2) Serial electron micrographs illustrate the selective presynaptic accumulation of CB_1 in boutons (b+), which form mainly asymmetric (flanked by black arrowheads) and sometimes symmetric (white arrowheads) synapses with dendrites (d) and spine heads (s). CB_1 staining remained under detection threshold in a few axon terminals (b−), which highlights quantitative differences in CB_1 expression between terminal types innervating the CeAL. (H–I) The anatomical nature of the synapse type is illustrated at higher magnification. Scale bars: A, B, D, E are 200 μm; C is 50 μm; F is 20 μm; G_1, G_2, H, I are 100 nm.

NIH-PA Author Manuscript
NIH-PA Author Manuscript
NIH-PA Author Manuscript

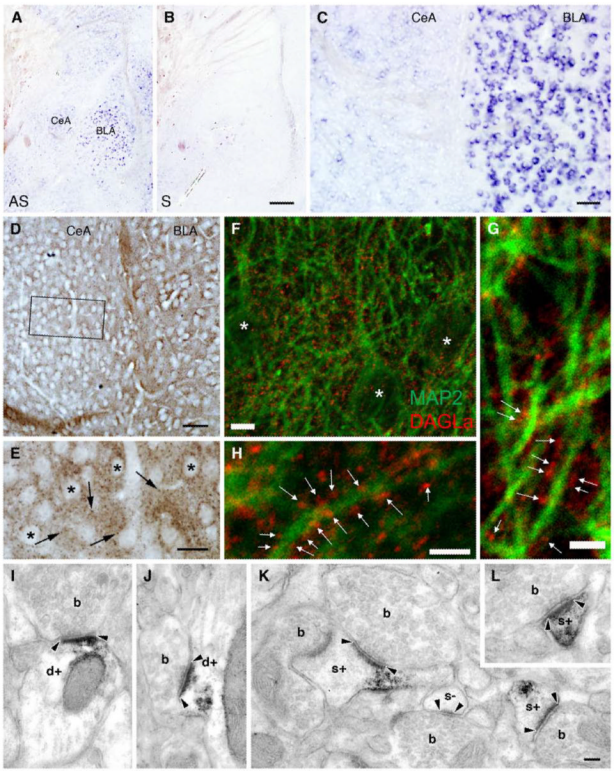

Figure 2. DAGLα is a Postsynaptic Enzyme in the CeAL

(A–B) *In situ* hybridization demonstrates the expression of DAGLα mRNA in both the BLA and CeA. AS and S depicts experiments performed by antisense and sense riboprobes, respectively. (C) Expression of DAGLα mRNA is notably higher in the BLA compared to the CeA. (D) However, at the protein level there is less difference between the two regions. (E) High magnification of the boxed region in D reveals that granular DAGLα-immunoreactivity (labeled by arrows) is present in the neuropil among cell bodies. (F–H) Confocal immunofluorescence analysis shows that DAGL α - immunoreactivity (red puncta indicated by white arrows) outlines MAP2-positive dendritic profiles (green). Asterisks denote CeAL cell bodies. (I–L) Electron micrographs provide ample evidence for the postsynaptic localization of DAGLα. Immunoreactivity represented by the black diaminobenzidine (DAB) precipitate was often present in dendrites (d+) and spine heads (s+), but never in boutons (b). Black arrowheads indicate the edge of the asymmetric synapses. Black arrowheads highlight asymmetric synapses. Scale bars: A–B are 200 μm; C–D are 50 μm; E is 20 μm; F is 5μm; G–H are 2.5μm; I–L are 100 nm.

NIH-PA Author Manuscript

NIH-PA Author Manuscript

NIH-PA Author Manuscript

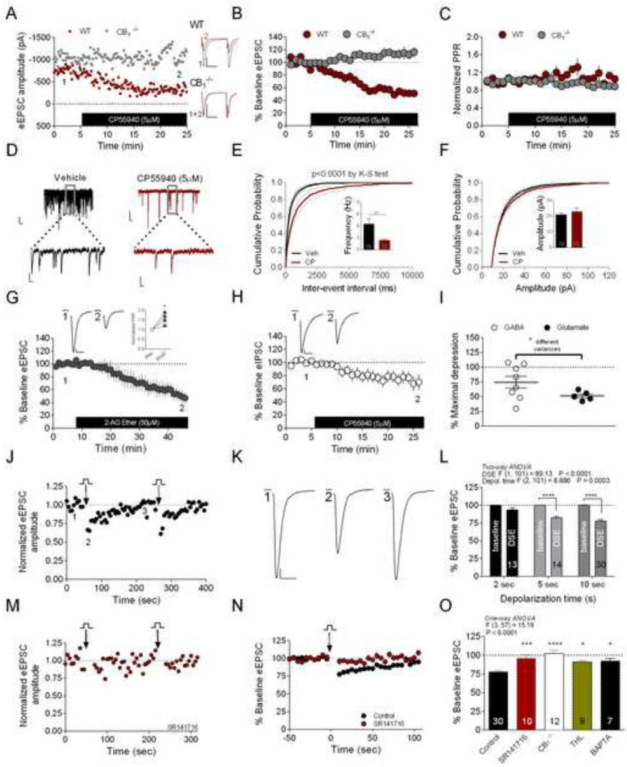

Figure 3. CB_1 Receptors Modulate Glutamate Release in the CeAL

(A–C) CP55940 depresses eEPSC amplitude in WT but not $CB_1^{-/-}$ mice, but does not affect PPR. (D–F) CP55940 reduces sEPSC frequency (E) but not amplitude (F). (G) 2-AG-ether depresses eEPSC amplitude and increases PPR (inset). (H) CP55940 decreases eIPSC amplitude. (I) Comparison of CP55940 effects on eIPSC and eEPSC amplitude. (J–L) Effects of postsynaptic depolarization on eEPSC amplitude; DSE in representative cell (J–K), and summary data of DSE after 2, 5 or 10 seconds of postsynaptic depolarization relative to corresponding baseline (L). (M–N) Effects of SR141716 on DSE after 10- second depolarization. (O) Summary data showing effects of SR141716, CB_1 deletion, THL, and intracellular BAPTA loading on DSE magnitude relative to control 10 second DSE. Control group in (O) represents the same data set as 10 second depolarization in (L). *p<0.05, **p<0.01, ***p<0.001, ****p<0.0001. Numbers of tested cells are indicated in bars for this and subsequent figures. Calibration scale bars in (A): 200pA, 25ms. Calibration scale bars for sEPSCs (D) at lower magnification (10pA, 100ms) and higher magnification (10pA, 20ms). All other scale bars: 10ms, 100pA. Data presented as mean ± SEM. Also see Figure S1.

NIH-PA Author Manuscript

NIH-PA Author Manuscript

NIH-PA Author Manuscript

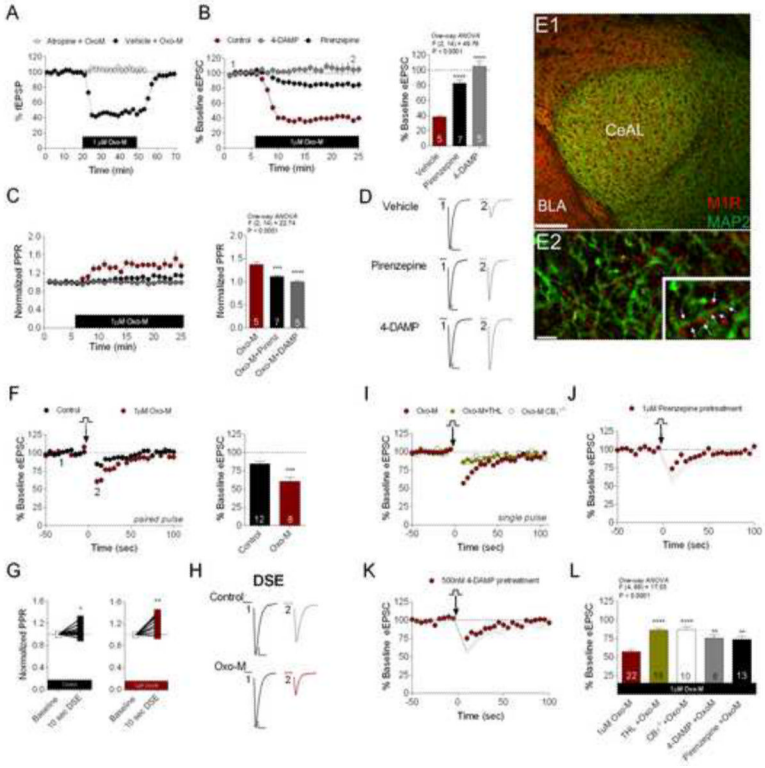

Figure 4. mAChRs Modulate Glutamate Release and Enhance DSE

(A) 1 μM Oxo-M depresses fEPSP amplitude, which is blocked in the presence of atropine. (B) Oxo-M-induced eEPSC depression is blocked by pirenzepine and 4-DAMP pretreatment. (C) Oxo-M increases PPR, which is blocked by pirenzepine and 4-DAMP pretreatment. (D) Representative traces of Oxo-M-induced eEPSC depression under vehicle, pirenzepine and 4-DAMP conditions. (E) Distribution of M_1 receptor (red) and the dendritic marker MAP2 (green) in the CeAL at low magnification; higher magnification shows punctate M1 staining in close apposition to MAP2 positive dendritic shafts (arrows in inset) (E1; scale bar 100μm, E2; bar 5μm, inset 7.5μm). (F) 1μM Oxo-M enhances DSE induced by 10 second depolarization. (G) PPR is increased by 10 second depolarization in both control and Oxo-M conditions. (H) Representative traces of control and Oxo-M DSE. (I) DSE in the presence of OXO-M is attenuated by THL and in $CB_1^{-/-}$ mice. (J–K) Effects of pirenzepine and 4-DAMP on DSE in the presence of 1μM Oxo-M; grey faded lines represent Oxo-M only DSE condition from (I) for visual comparison purposes. (L) Summary data of the effects of THL, CB_1 deletion, pirenzepine, and 4-DAMP on 10 second DSE in the presence of Oxo-M. **p<0.01, ***p<0.001, ****p<0.0001. Scale bars: 10ms, 100pA. Data presented as mean ± SEM. Also see Figure S2.

NIH-PA Author Manuscript

NIH-PA Author Manuscript

NIH-PA Author Manuscript

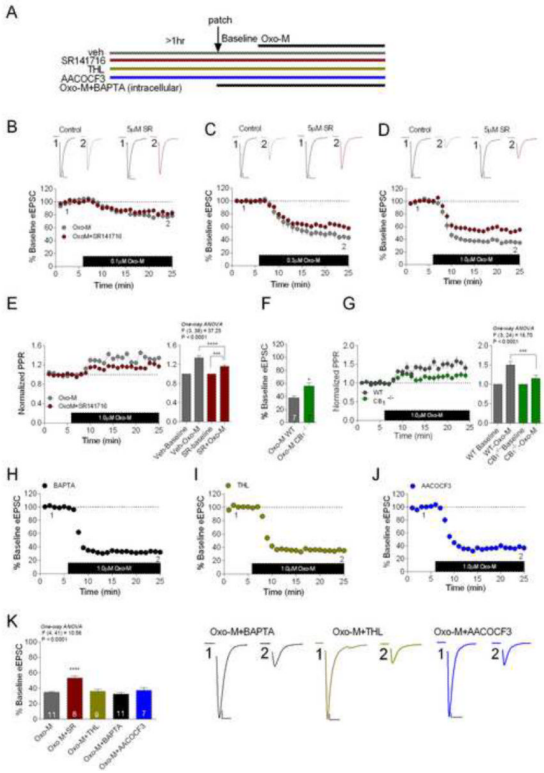

Figure 5. Acute mAChR Activity Drives Ca^{2+}-and DAGL-*Independent* eCB Release

(A) Diagram of experimental design. (B–D) Oxo-M induced eEPSC depression is partially blocked by SR141716 at 0.3μM and 1 μM Oxo-M conditions. (E) 1 μM Oxo-M-induced increase in PPR is attenuated by SR141716; residual depression in the presence of SR141716 is associated with a residual increase in PPR. (F) 1μM Oxo-M induced eEPSC depression is attenuated in $CB_1^{-/-}$ mice. (G) The increase in PPR after Oxo-M application is attenuated in $CB_1^{-/-}$ mice. (H–K) Effects of BAPTA (H), THL (I), and the PLA2 inhibitor AACOCF3 (J), on 1μM Oxo-M-induced eEPSC depression. (K) Bar graph and representative traces of summary data depicting the effects of SR141716, THL, BAPTA, and AACOCF3 on 1μM Oxo-M-mediated maximal eEPSC depression. *p<0.05, ***p<0.001, ****p<0.0001. Scale bars: 10ms, 100pA. Data presented as mean ± SEM.

NIH-PA Author Manuscript

NIH-PA Author Manuscript

NIH-PA Author Manuscript

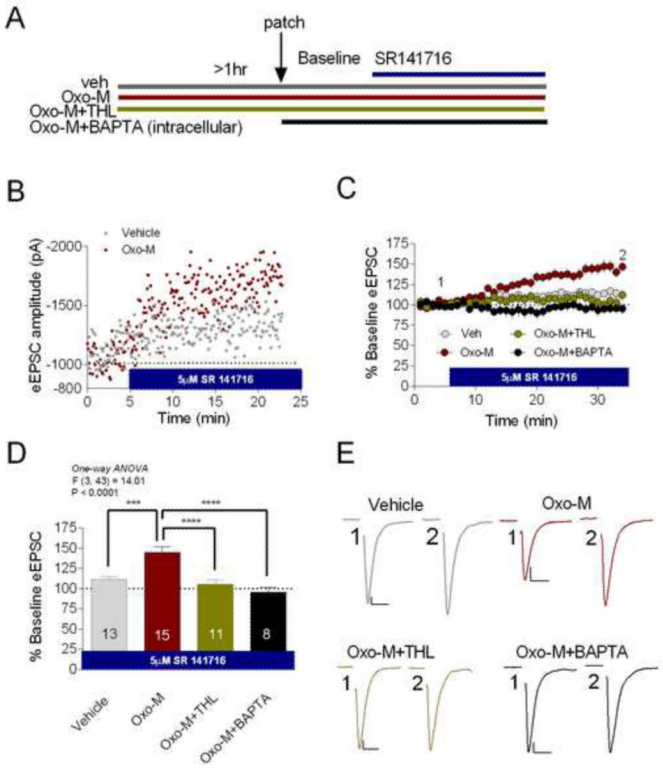

Figure 6. Persistent mAChR Activity Drives Ca^{2+} - and DAGL-*Dependent* eCB Release

(A) Diagram of experimental design. (B–C) Representative cells and group data showing that in the continuous presence of Oxo-M, SR141716 causes synaptic potentiation relative to vehicle conditions. (C) Co-incubation of THL and Oxo-M prevents SR141716-induced synaptic potentiation, as does intracellular BAPTA loading. (D) Summary data showing the effects of SR141716 under vehicle, Oxo-M, Oxo-M+THL, and Oxo-M+BAPTA pre-treatment conditions. (E) Representative traces of summary data in (D). ***p<0.001, ****p<0.0001. Scale bars: 10ms, 100pA. Data presented as mean ± SEM.

NIH-PA Author Manuscript

NIH-PA Author Manuscript

NIH-PA Author Manuscript

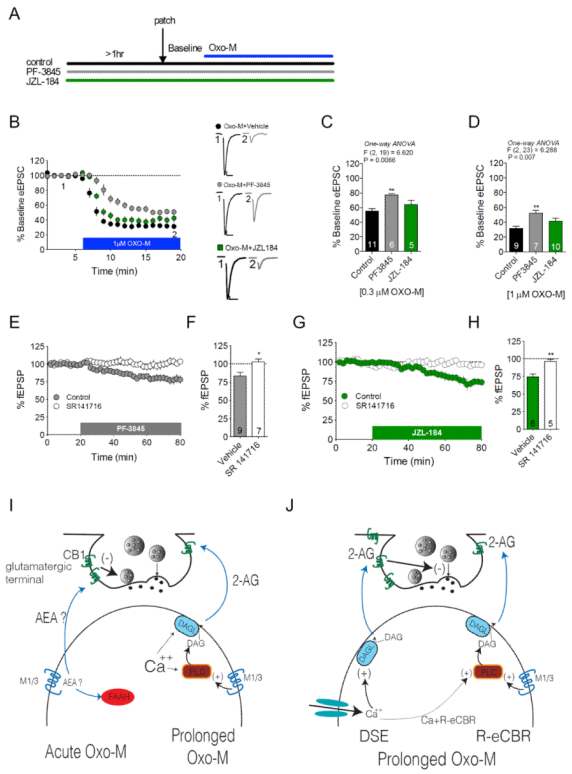

Figure 7. Acute mAChR Receptor Activity Drives Synaptic AEA Signaling

(A) Experimental design for B–D. (B–D) Oxo-M-induced acute synaptic depression (0.3 μM and 1 μM) is partially occluded by the FAAH inhibitor PF-3845, but not the MAGL inhibitor JZL-184; time-course for 1μM Oxo-M condition shown in (B). (E–F) Effects of PF-3845 on synaptic depression under control or CB_1 antagonist pretreatment conditions. (G–H) Effects of JZL-184 on synaptic depression under control or CB_1 antagonist pretreatment conditions. (I) Diagrammatic representation of differences between acute vs. prolonged mAChR activation with Oxo-M. Acute Oxo-M application induces a short-lived "burst" of AEA to reduce afferent glutamate release, while prolonged mAChR activation causes a tonic calcium- and DAGL-dependent 2-AG release. (J) During prolonged mAChR activation, tonic 2-AG release continues and calcium-assisted mAChR-driven 2-AG release is induced by co-incident postsynaptic depolarization (i.e. DSE enhancement in the presence of continuous Oxo-M). Ca+R-eCBR: calcium-assisted receptor driven eCB release; *p<0.05, **p<0.01. Scale bars: 10ms, 100pA. Data presented as mean ± SEM. Also see Figure S3.